Supporting information to

Continuous-flow Production of Perfluorocarbon-loaded Polymeric Nanoparticles: from the Bench towards the Clinic

Esmee Hoogendijk[1], Edyta Swider[1,§], Alexander H. J. Staal[1,§], Paul B. White[2], N. Koen van Riessen[1], Gunnar Glaßer[3], Ingo Lieberwirth[3], Anna Musyanovych,[4] Christophe A. Serra[5], Mangala Srinivas[1,#,], Olga Koshkina[1,3,#,*]*

[1]Department of Tumor Immunology, Radboud Institute for Molecular Life Sciences, Radboud University Medical Center, Geert Grooteplein 26/28, 6525GA, Nijmegen, The Netherlands

[2]Institute for Molecules and Materials, Radboud University, Nijmegen, The Netherlands

[3]Max Planck Institute for Polymer Research, Ackermannweg 10, 55128 Mainz, Germany

[4]Fraunhofer IMM, Carl-Zeiss Str. 18-20, 55129 Mainz, Germany

[5]Université de Strasbourg, CNRS, Institut Charles Sadron, 23 rue du Loess, F- 67083 Strasbourg, France

Corresponding Author

*koshkina@mpip-mainz.mpg.de

*mangala.srinivas@radboudumc.nl

Content

1. Effect of different parameters of synthesis on nanoparticle characteristics

1.1. Impact of ratio PFCE / organic phase

Table S1. Flow rates and characterization of PFCE-PLGA nanoparticles (DCM as a solvent) with NMR and DLS (Q_{total} = 25 ml min^{-1}).

Sample	Q_{PFC} (mL/min)	Q_{PLGA} (mL/min)	Q_{PVA} (mL/min)	Q_{PFC} / Q_O	R_h (nm)	PDI	PFCE content (wt.-%)
PFCE6	0.83	4.17	20	0.2	174	0.16	22
PFCE3	1.15	3.85	20	0.3	180	0.17	28
PFCE7	1.43	3.57	20	0.4	166	0.24	23
PFCE8	1.87	3.13	20	0.6	179	0.21	22
PFCE9	2.5	2.5	20	1	171	0.23	26

1.2. Impact of ratio mixture 1 / aqueous phase

Table S2. Flow rates and characterization of PFCE-PLGA nanoparticles (DCM as a solvent) with NMR and DLS (Q_{total} = 25 mL min^{-1}, Q_{PFC}/Q_{PLGA} = 0.3).

Sample	Q_{PFC} (mL/min)	Q_{PLGA} (mL/min)	Q_{PVA} (mL/min)	Q_{M1}/Q_{PVA}	R_h (nm)	PDI	PFCE content (wt.-%)
PFCE1	0.64	2.14	22.22	0.125	181	0.19	26
PFCE2	0.82	2.75	21.43	0.167	188	0.19	28
PFCE3	1.15	3.85	20	0.25	180	0.17	28
PFCE4	1.44	4.81	18.75	0.33	167	0.21	21
PFCE5	1.92	6.42	16.66	0.50	168	0.19	19

1.3. Impact of total flowrate

Table S3. Flow rates and characterization of PFCE-PLGA nanoparticles made with DCM as solvent (Figure 1b; Q_{PFC}/Q_{PLGA} = 0.3, Q_{MI}/Q_{PVA} = 0.25).

Sample	Q_{PFC} (mL/min)	Q_{PLGA} (mL/min)	Q_{PVA} (mL/min)	R_h (nm)	PDI	PFCE content (wt.-%)
PFCE10	0.29	0.97	5	171	0.17	16
PFCE11	0.29	0.97	5	164	0.2	20
PFCE12	0.58	1.93	10	190	0.12	23
PFCE13	0.58	1.93	10	167	0.23	29
PFCE14	0.87	2.9	15	191	0.16	35
PFCE15	0.87	2.9	15	194	0.18	31
PFCE16	1.15	3.85	20	193	0.13	30
PFCE3	1.15	3.85	20	180	0.17	28
PFCE17	1.44	4.81	25	172	0.2	30
PFCE18	1.44	4.81	25	169	0.2	25
PFCE19	1.73	5.78	30	152	0.17	27
PFCE20	1.73	5.78	30	141	0.18	28

1.4.Impact of type of perfluorocarbon on PFC-PLGA nanoparticles

Table S4. Flow rates and characterization of PFOB-PLGA nanoparticles made with DCM as solvent (in Figure 1c and Figure 5).

Sample	Q_{PFC} (mL/min)	Q_{PLGA} (mL/min)	Q_{PVA} (mL/min)	R_h (nm)	PDI	PFOB content (wt.-%)
PFOB1	0.58	1.93	10	194	0.31	42
PFOB2	0.58	1.93	10	199	0.36	38
PFOB3	0.87	2.9	15	183	0.31	54
PFOB4	0.87	2.9	15	189	0.31	44
PFOB5	1.15	3.85	20	191	0.27	52
PFOB6	1.15	3.85	20	166	0.25	49
PFOB7	1.44	4.81	25	163	0.21	61
PFOB8	1.44	4.81	25	157	0.27	55
PFOB9	1.73	5.78	30	130	0.2	52
PFOB10	1.73	5.78	30	143	0.2	52

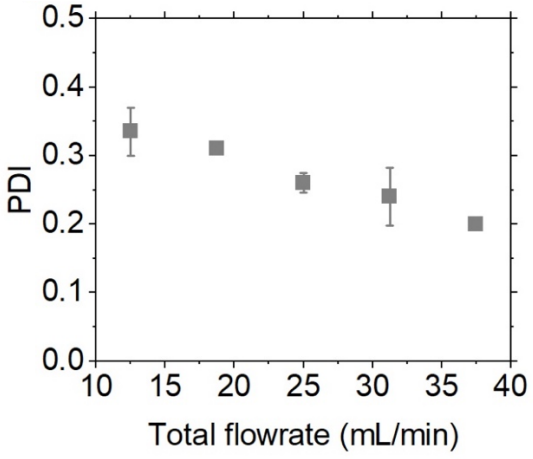

Figure S1. PDI of PFOB-PLGA nanoparticles. An increase of flow rates results in a smaller PDI. All batches are repeated once

1.5. Impact of type of solvent

Table S5. Flow rates and characterization of PFCE-PLGA nanoparticles from Figure 2.

Sample	Organic solvent	Q_{PFC} (mL/min)	Q_{PLGA} (mL/min)	Q_{PVA} (mL/min)	R_h (nm)	PDI	PFCE content (wt.-%)
PFCE13	DCM	0.58	1.93	10	167	0.23	29
PFCE3	DCM	1.15	3.85	20	180	0.17	28
PFCE20	DCM	1.73	5.78	30	141	0.18	28
PFCE21	Chloroform	0.58	1.93	10	168	0.25	35
PFCE22	Chloroform	1.15	3.85	20	162	0.2	42
PFCE23	Chloroform	1.73	5.78	30	136	0.12	36
PFCE24	DCM/MeCN	0.58	1.93	10	139	0.18	9
PFCE25	DCM/MeCN	1.15	3.85	20	126	0.14	10
PFCE26	DCM/MeCN	1.73	5.78	30	112	0.11	9
PFCE27	AcOEt	0.58	1.93	10	114	0.23	9
PFCE28	AcOEt	1.15	3.85	20	96	0.08	3
PFCE29	AcOEt	1.73	5.78	30	87	0.11	2

1.6.Continuous large-scale production of nanoparticles

Table S6. Flow rates and characterization of PFCE-PLGA nanoparticles (DCM as solvent) produced during longer run.

Fraction	Q_{PFC} (mL/min)	Q_{PLGA} (mL/min)	Q_{PVA} (mL/min)	R_h (nm)	PDI	PFCE content (wt.-%)
PFCE30A	1.15	3.85	20	172	0.21	33
PFCE30B	1.15	3.85	20	176	0.20	30
PFCE30C	1.15	3.85	20	169	0.18	31
PFCE30D	1.15	3.85	20	174	0.17	31
PFCE30E	1.15	3.85	20	172	0.21	30
Average				173	0.19	31
Std. deviation (%)				1.3	8.5	3.6

Table S7. Flow rates and characterization of different fractions of PFCE-PLGA nanoparticles (chloroform as a solvent) from longer run.

Fraction	Q_{PFC} (mL/min)	Q_{PLGA} (mL/min)	Q_{PVA} (mL/min)	R_h (nm)	PDI	PFCE content (wt.-%)
PFCE31A	1.44	4.81	25	187	0.30	45
PFCE31B	1.44	4.81	25	188	0.33	44
PFCE31C	1.44	4.81	25	179	0.28	45
Average				185	0.30	45
Std. deviation (%)				2.2	6.8	1.1

Operation stability over longer period of time

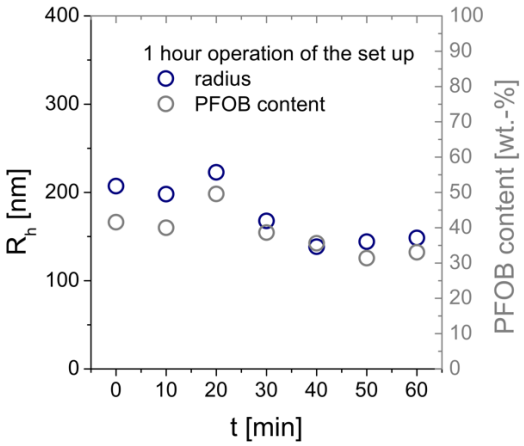

Figure S2. Operation of the set-up for one hour tested with PFOB as cargo at flowrates Q_{PVA} = 20mL min^{-1}, Q_{PLGA} = 3.85 mL min^{-1}, Q_{PFOB} = 1.15 mL min^{-1}. The PDI values were between 0.2 and 0.3 similar, as in a shorter run. Nanoparticles were isolated by centrifugation and freeze-dried prior analysis.

We accessed the performance of the set up over a longer period of time for the production of PFOB-PLGA nanoparticles. The set up was operated for one hour, and the fractions were collected for purification and analysis every 10 minutes. The standard deviation of radius was 18% and the standard deviation of PFOB content was 15%. This deviation is comparable to the batch production. It shows that the implementation of quality control mechanisms is necessary prior the use of the set up for the production of larger amounts of nanoparticles. Ideally, the set up should be extended with online detection and online purification methods for the large-scale process. All fractions had PFOB content above 30 wt.-% showing that they are suitable for ^{19}F MRI applications. Thus, even with the given variation between the fractions the continuous method is less work intensive than the batch method and allows to obtain higher yields in a shorter time.

2. Additional cell and imaging data

2.1. Characteristics of nanoparticles used for MTT assay

Table S8. Flow rates and characterization of PFCE-PLGA nanoparticles in Figure 4a and S2

ID in Figure 4a or S2	Sample	Organic solvent	Q_{PFC} (mL/min)	Q_{PLGA} (mL/min)	Q_{PVA} (mL/min)	R_h (nm)	PDI	PFCE content (wt.-%)
DCM 1	PFCE12	DCM	0.58	1.93	10	190	0.12	23
DCM 2	PFCE16	DCM	1.15	3.85	20	193	0.13	30
DCM 3	PFCE19	DCM	1.73	5.78	30	152	0.17	27
$CHCL_3$ 1	PFCE32	Chloroform	0.58	1.93	10	157	0.31	34
$CHCL_3$ 2	PFCE33	Chloroform	1.15	3.85	20	171	0.26	46
$CHCL_3$ 3	PFCE34	Chloroform	1.73	5.78	30	150	0.23	40

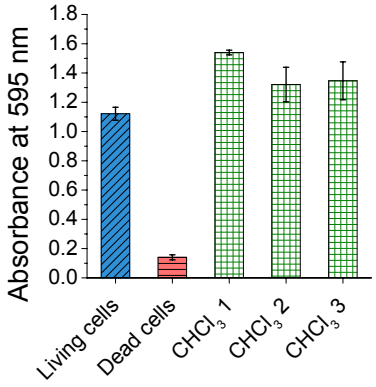

Figure S3. Cell viability assay after incubation with PFCE-PLGA chloroform nanoparticles for 24 hours.

2.2. Characterization of nanoparticles loaded with Atto-647 for confocal imaging

Table S9. Flow rates and characterization of DCM PFCE-PLGA nanoparticles used for cellular uptake studies (Figure 4b and S3 and S4)

Sample	Q_{PFC} (mL/min)	Q_{PLGA} (mL/min)	Q_{PVA} (mL/min)	R_h (nm)	PDI	PFCE content (wt.-%)
PFCE35[a]	1.15	3.85	20	163	0.27	38
PFCE36	1.44	4.81	25	162	0.30	42
PFCE37	1.73	5.78	30	128	0.17	39

[a] used in Figure 4b

2.3.Confocal microscopy of cells after nanoparticle uptake

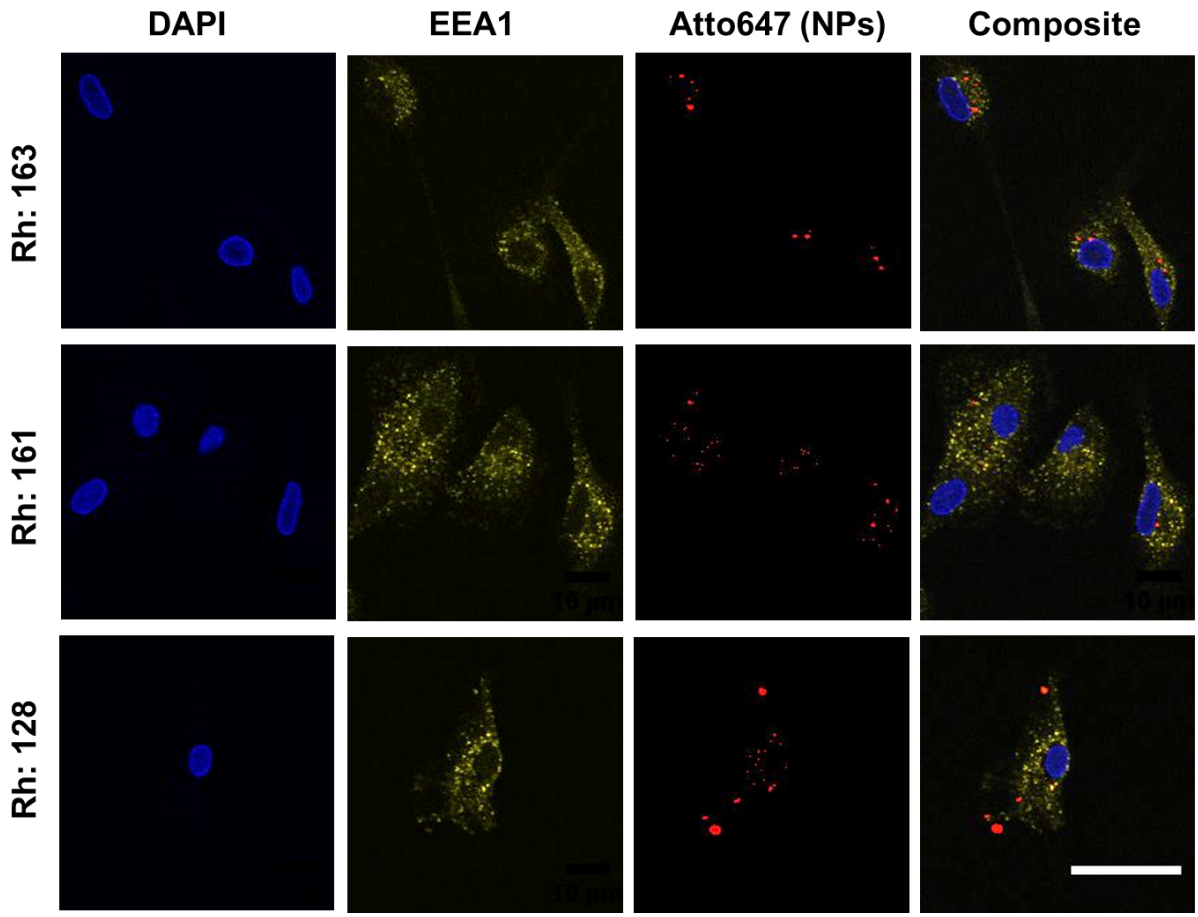

Figure S4. Confocal microscopy images with EEA1 staining. Scale bar: 25 μm. Images are processed with ImageJ.

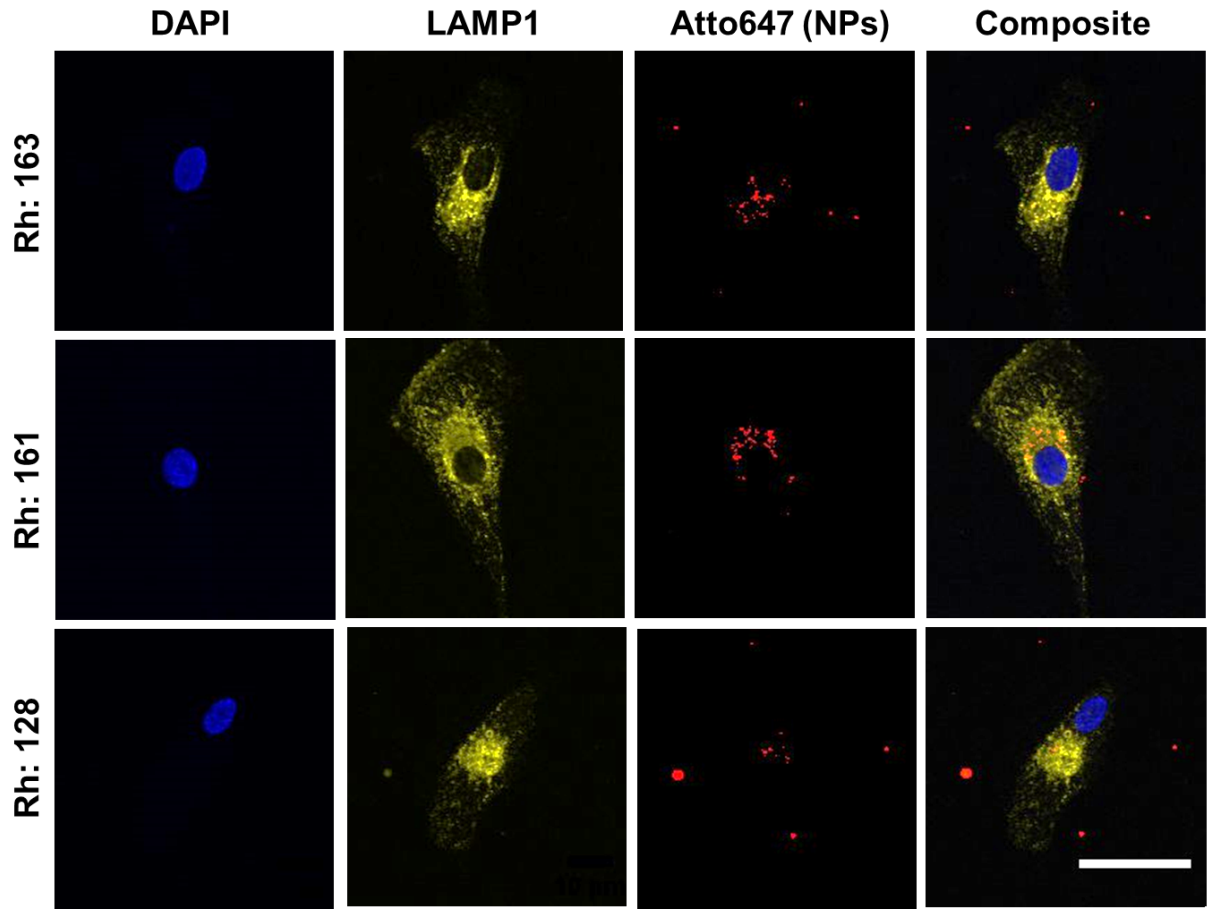

Figure S5. Confocal microscopy images with LAMP1 staining. Scale bar 25 μm. Images are processed with ImageJ.

2.4. ^{19}F MRI and Ultrasound in vitro

Table S10. Characteristics of PFC-PLGA nanoparticles used for 19F MRI imaging in Figure 4d and S6.

Nr. in Figure	Sample	Organic solvent	Q_{PFC} (mL/min)	Q_{PLGA} (mL/min)	Q_{PVA} (mL/min)	R_h (nm)	PDI	PFC content (wt.-%)
1	PFCE21	Chloroform	0.58	1.93	10	168	0.25	35
2	PFCE22	Chloroform	1.15	3.85	20	162	0.20	42
3	PFCE23	Chloroform	1.73	5.78	30	136	0.12	36
4	PFOB1	DCM	0.58	1.93	10	194	0.31	42
5	PFOB5	DCM	1.15	3.85	20	191	0.27	52
6	PFOB9	DCM	1.73	5.78	30	140	0.20	52
7	PFCE12	DCM	0.58	1.93	10	190	0.12	23
8	PFCE16	DCM	1.15	3.85	20	193	0.13	30
9	PFCE19	DCM	1.73	5.78	30	152	0.17	27

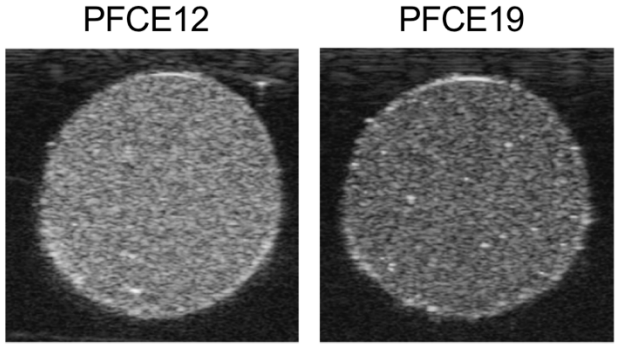

Figure S6. Ultrasound images showing the signal of various nanoparticle suspensions. Nanoparticles in suspension placed in a gel phantom show acoustic contrast to the surrounding gel. Nanoparticles presented here were produced with DCM. Water was used as a negative control. c(NP) = 10 mg mL^{-1}

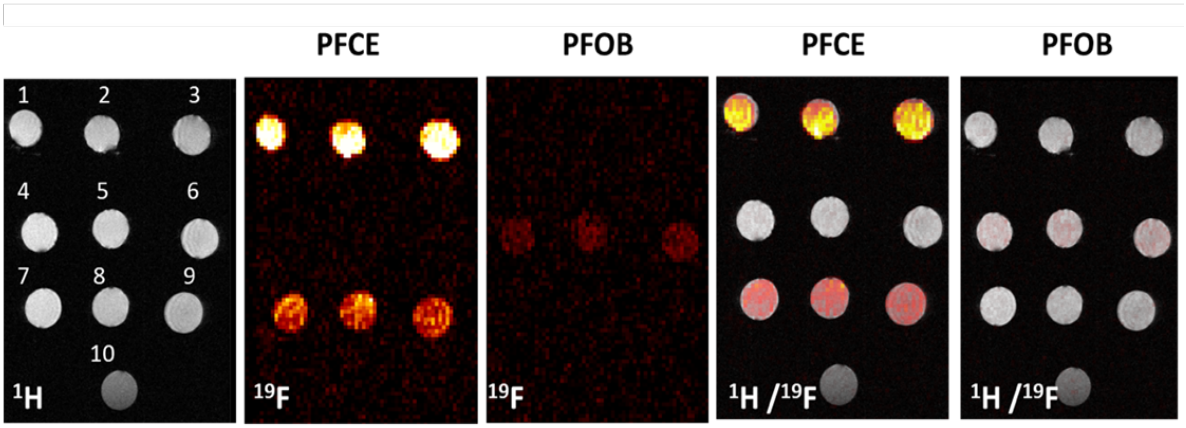

Figure S7. ^{19}F MRI images of aqueous dispersions of PFCE-nanoparticles produced either with chloroform (first row) or DCM (third row) and PFOB nanoparticles (mid row). c(NP) = 10 mg mL^{-1}, 11.7 T, 3D RARE sequence.

Table S11. Signal-to-noise ratio ^{19}F MRI.

# in Figure 6A	NP name	Solvent	SNR	Average SNR
1	PFCE21	Chloroform	10.1	
2	PFCE22	Chloroform	9.7	10.2
3	PFCE23	Chloroform	10.7	
4	PFOB1	DCM	2.9	
5	PFOB5	DCM	2.6	2.6
6	PFOB9	DCM	2.4	
7	PFCE12	DCM	6.3	
8	PFCE16	DCM	6.4	6.2
9	PFCE19	DCM	6.0	
10	Control – water	-	0.9	

The differences in signal intensity can be attributed to a different encapsulation of PFC. Since PFOB displays several NMR signals, only some of the ^{19}F nuclei of PFOB can be imaged with conventional sequence without chemical shift artifacts. Therefore, the images of PFOB nanoparticles have lower signal intensity than the PFCE nanoparticles, despite the fact that they

have higher PFC encapsulation. Furthermore, with the PFCE-PLGA nanoparticles made with chloroform, an average signal-to-noise ratio of 10 could be obtained in just 45 seconds of imaging, which is comparable to PFCE-PLGA nanoparticles made with the conventional batch method (Table S12). Both concentration and imaging time used here are applicable for the imaging *in vivo*.

2.5. ^{19}F MRI *in vivo* at different timepoints

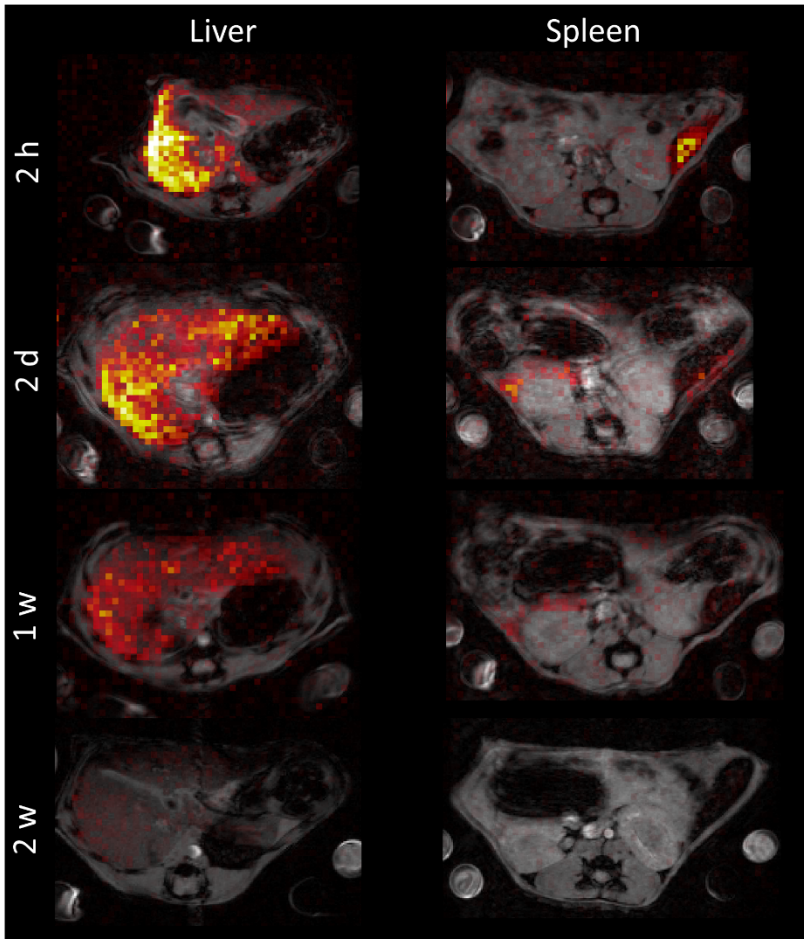

Figure S8. In vivo ^{19}F MRI images of liver and spleen. Liver and spleen were imaged at different time points to check for the presence of ^{19}F signal.